Surface Tension Propellant Acquisition System Technology for Space Shuttle Reaction Control Tanks

Dale A. Fester,* Ashton J. Villars,† and Preston E. Uney†
Martin Marietta Corporation, Denver, Colo.

A program was conducted to provide the technology base for the Space Shuttle Reaction Control System (SS/RCS) flight tankage. Through a combination of analysis, subscale testing, and computer predictions, a surface tension acquisition/expulsion system design was developed for the Orbiter RCS application. A full-scale tank system was fabricated and ground verification testing was conducted. Cleaning, inspection, fill and drain, and 1-*g* expulsion performance were demonstrated. Results show that the fine-mesh screen, compartmented tank system should provide the performance, flexibility, reusability, and other characteristics required by the pulsing, high flowrate RCS. The required expulsion under widely differing high *g* boost abort and re-entry vectors oriented 119° apart and during on-orbit operation under omnidirectional low *g* conditions should be obtained.

Introduction

SURFACE tension propellant acquisition/expulsion devices have been flight proven on several Earth-orbital and interplanetary vehicles for both monopropellant and bipropellant systems. Many others have been built and tested or are in the conceptual stage. Each of these devices was designed to perform to a unique set of operational requirements and environmental conditions; there is not one universal design that will satisfy all mission criteria for all applications. This is particularly true for the Space Shuttle Reaction Control System (SS/RCS), where a new design is needed to meet a completely new and demanding set of requirements and conditions.

The SS/RCS components have as requirements/goals: 1) 30-day operation for 100-mission life with minimum maintenance; 2) capability for servicing, loading, and unloading both on and off the orbiter; 3) simple and insensitive checkout and servicing procedures; and 4) liquid propellant supply to the engines without pressurant gas ingestion. With its passive nature, all-metal surface tension tankage was the most promising acquisition/expulsion method to meet these requirements/goals and it was selected as the baseline system. This is also true for the orbital maneuvering system (OMS).

The RCS bipropellant propulsion system, using N_2O_4 and monomethylhydrazine (MMH) at the equal volume mixture ratio of 1.65, performs attitude control and small ΔV translational maneuvers. It consists of a single forward module in the nose of the orbiter and two aft modules located in the OMS pods at each side of the tail. The forward module contains one oxidizer and one fuel tank and a pressurization system; it supplies a total of 22 thrusters (8 primary and 3 vernier on each side) in the nose of the orbiter which are used for on-orbit operation only. Each aft module also contains one oxidizer and one fuel tank that supply a total of 12 thrusters; there are a total of 24 RCS thrusters at the rear of the orbiter. These thrusters are used on-orbit, provide all RCS accelerations in the $+X$ direction, are used in the event of boost abort, and supply all RCS demands during re-entry. For this study, the tanks are spherical, 38 in. diam and are pressurized with helium to a nominal operating pressure of 280 psia. Maximum propellant load is 1343 lbm N_2O_4 and 840 lbm MMH; minimum load is 65% of this value. The propellant temperature range is 40-125°F and flowrate per thruster is 2.19 lbm/sec N_2O_4 and 1.32 lbm/sec MMH.

RCS operation is not required during a normal boost sequence. However, all aft module engines are fired during the return-to-launch-site (RTLS) boost abort operations to deplete all but 34.5% of tank capacity (753 lbm of propellant) that is required for re-entry. RTLS abort imposes the worst conditions of high outflow rates (12 engines firing) and accelerations up to 3.3*g*. Re-entry imposes another high-*g*, high outflow condition (2.2*g*, 9 engines/firing) which tends to conflict with the RTLS requirements, having an acceleration vector up to 119 deg from the RTLS vector. The propellant required for re-entry is between 13 and 34.5% of the tank capacity, depending on the particular mission and trajectory flown, and high expulsion efficiency is desired. Furthermore, re-entry must be accomplished without relying on surface tension acquisition when accelerations are greater than 0.05*g*. Final RTLS and re-entry liquid orientations are shown in Fig. 1 to display the difficulty of locating a tank outlet with the high *g* vectors separated by up to 119 deg. The most desirable location for the outlet is toward the $+Z$ side of the tank at the edge of both puddles.

High outflow rates are required at relatively high acceleration levels during on-orbit operations (10 engines firing to produce a maximum omnidirectional acceleration of 0.231*g*). In addition, the OMS engines produce random vibrations of 1.93*g* rms which act on the aft RCS tanks. If one OMS engine fails, four aft RCS thrusters will be operated to maintain orbiter attitude while using the remaining OMS engine.

This application presents the most stringent requirements ever placed on a surface tension system. Because of the difficult nature of these sometimes conflicting requirements, a program was undertaken to provide the technology and insight needed for the flight hardware RCS surface tension

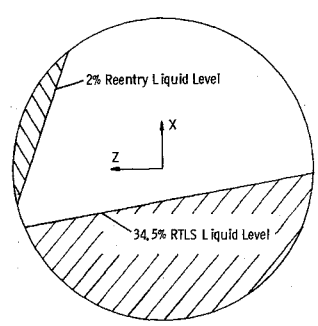

Fig. 1 RTLS and re-entry liquid puddle orientations.

Presented as Paper 75-1196 at the AIAA/SAE 11th Propulsion Conference, Anaheim, California, Sept. 29-Oct. 1, 1975; submitted Sept. 29, 1975; revision received March 22, 1976. This work was performed under Contract NAS9-13709.

Index categories: Liquid Rocket Engines; Spacecraft Attitude Dynamics and Control; Spacecraft Propulsion Systems Integration.

*Unit Head, Aerothermal and Propulsion Department. Member AIAA.

†Engineer, Aerothermal and Propulsion Department.

tankage program. The specific objective of this technology program was to analyze, design, fabricate, and test surface tension propellant acquisition/expulsion tankage that satisfies the requirements of the SS/RCS.

An earlier paper[1] presented the rationale leading to the selection of a compartmented tank with individual screen flow channels in both the pressurization compartment and the outlet compartment as the preferred surface tension concept for the SS/RCS. This paper encompasses the development phase of the program, which includes subscale concept verification and full-scale tankage evaluation.

Concept Verification

Concept Design

Analysis of the selected acquisition concept was performed to define the preliminary system design shown in Fig. 2. The design approach included a safety factor of 1.5 on bubble point; common design for all tanks; complete draining of the pressurization compartment in low g; common channel cross-section in both compartments; and single layer, 325×2300 mesh, Dutch-twill screen. Rationale for this approach is presented in Ref. 1.

With this device, a single barrier divides the tank into the two compartments, as shown in Fig. 2. Propellant is fed through the channels of the pressurization compartment into the manifold, through the barrier window, to the bulk region of the outlet compartment. From here, it flows into the channels of the outlet compartment to the tank outlet. With this arrangement, the channels of the pressurization compartment can feed two-phase fluid to the outlet compartment. The pressurization compartment must be depleted prior to the outlet compartment to maximize the on-orbit expulsion efficiency of the forward module. A near-zero residual is possible because, even after breakdown the pressurization compartment channels continue to scavenge propellant, transferring a gas-liquid mixture to the outlet compartment.

Channel number, size, shape, and barrier position were optimized, using the surface tension system computer model developed for this program, to provide maximum on-orbit expulsion efficiency η_e under 0.231 g omnidirectional acceleration. The cases of liquid puddled over a single channel or between two channels were considered for various acceleration vectors. Flow area and aspect ratio were varied for four, six, and eight channels. Four 9.5 in. $\times$ 0.75 in. channels were selected. Results, summarized in Fig. 3, show increased η_e at lower barrier positions. The barrier volume of 14% of tank volume was determined from screen stability considerations in the on-orbit environment of 0.231-g acceleration plus 1.93-g rms OMS engine vibration.

Barrier inclination and outlet location were determined by the conflicting high g aft tank RTLS and re-entry terminal drain requirements. A barrier angle of 16.5 deg with the outlet toward the $+Z$ axis and below the barrier was considered sufficient to place the outlet within the reentry puddle while keeping the outlet compartment submerged, precluding screen dryout, during RTLS boost abort outflow to 34.5% of liquid load. A single screen window, located on the $+Z$ side of the tank, provided the liquid flow path from pressurization to outlet compartment. A coarser 165×800 mesh Dutch-twill screen provided adequate liquid retention capability and kept the flow losses through the window to a minimum. A channel manifold was also used to gain additional screen area (Fig. 2). The weight of the device was estimated to be 22 lbm.

Verification Testing

The test program was conducted to verify the suitability of the surface tension system for SS/RCS application and to define required changes in design details. System performance was assessed for the various mission phases of ground operations, high-g RTLS boost abort, low-g orbital operations, and high-g re-entry. A 1/3 scale model was fabricated according to the preliminary design and used to verify system performance by scaling and by correlation with computer predictions. The model had Dutch-twill screen of 325×2300 mesh on the channels and manifolds and 80×700 mesh on the screen window. In addition, a 2/15 scale plastic tank was used to evaluate low-g liquid reorientation in a compartmented spherical tank.

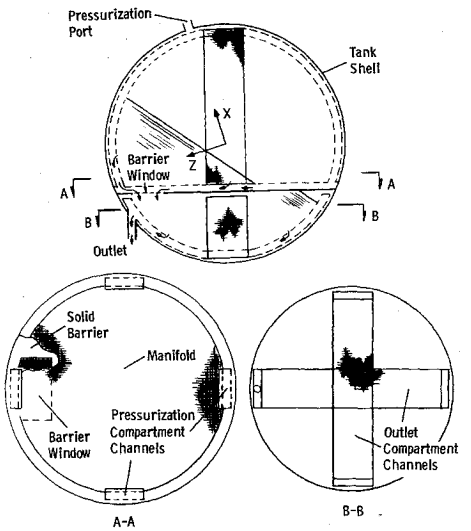

Fig. 2 Preliminary design

CURVE	CHANNEL WIDTH (IN.)	CHANNEL DEPTH (IN.)	CHANNEL AREA (IN^2)	BARRIER LEVEL (%)
A	13.4	0.5	6.7	34.5
B	9.6	0.7	6.7	34.5
C	6.7	1.0	6.7	34.5
D	9.5	0.75	7.1	16.5

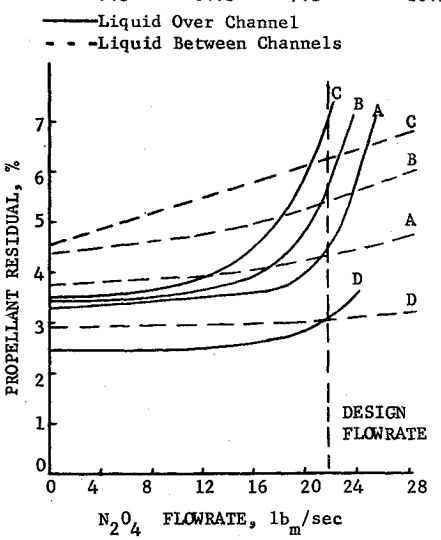

Fig. 3 Performance of various four-channel systems

Proper scaling is required in conducting model tests. In operation, the capillary retention capability of the screen, as determined by the bubble point, must offset all of the adverse pressure differentials of the flowing system. With a totally wetting fluid, this can be expressed as

$$\Delta P_c = 2\sigma/r = BP \tag{1}$$

and

$$BP \geq \Delta P_h + \Delta P_e + \Delta P_v + \Delta P_f + \Delta P_t \tag{2}$$

where ΔP_c = retention capability of screen, BP = bubble point of screen, σ = liquid surface tension, r = pore radius of screen, ΔP_h = hydrostatic head supported by screen, ΔP_e = pressure loss due to flow through screen, ΔP_v = change in pressure head to velocity head, ΔP_f = viscous loss due to flow in channel, and ΔP_t = loss due to transients, pulsed flow, vibration, etc. The ratio of the individual pressure loss terms to the bubble point should remain constant between the model and the prototype. Acceleration and flow rate scaling considered propellant and test fluid properties and the scale of the model.

Acceleration scaling maintained hydrostatic head similarity. By selecting the appropriate test fluid, acceleration was scaled to simulate the low-g and high-g mission events. Isopropyl alcohol (IPA) in a one-g environment with the ⅓ scale model simulated N_2O_4 on-orbit operations at 0.231 g. Freon TF with its higher density was selected for the high-g tests to keep test acceleration as low as possible. Flowrate scaling was based on the entrance, velocity, and friction loss terms. A single flowrate would not scale the relative magnitude of the pressure loss terms at breakdown because of the difference between propellant and test fluid properties and because ΔP_e varies linearly with the scale while ΔP_v and ΔP_f vary with the square of the scale (approximately). As a result, weighting factors were used with each pressure term, based on full-scale system pressure differentials at breakdown and keeping the summation of flow ΔP constant. Model expulsion at the resulting subscale flow rates then provides a direct indication of full-scale performance. Details of this scaling are presented in Ref. 2.

Testing to assess ground fill and drain, on-orbit expulsion, pulsed-flow effects, high-g RTLS and re-entry expulsion, vibration effects, and slosh was conducted with the ⅓ scale model. The fill-and-drain testing evaluated various techniques to accomplish these ground servicing operations. Test fluids were IPA and water. Wicking barriers located in the channel high points allowed venting of gas from inside the channels during filling and allowed the tank to be filled to any level with initially dry screens. The tank had to be filled completely, however, to fill the pressurization compartment channels. Filling with wet screens trapped large quantities of gas within the channels, nearly equal to the channel volume. Using a slow tank drain until screen breakdown and then increasing the driving pressure to force out a two-phase mixture resulted in successful drain to less than 1% liquid residual.

Over 175 expulsion tests were conducted with the model in a 1-g environment to evaluate expulsion performance during simulated on-orbit mission events and to allow comparison with computer predictions. The tests used IPA and focused on outlet compartment depletion. Tests were made with four tank attitudes of $+X$-axis up and down and $+Z$-axis up and down. Measured η_e as a function of flowrate for the $+X$ up orientation is shown in Fig. 4. Predicted performance is slightly conservative, but in good agreement with the experimental data. Depletion at the scaled high-mode N_2O_4 flowrate of 12.2 in.^{3}/sec shows a measured η_e of 97.8%. The low-mode flowrate of 3.7 in.^{3}/sec is below the range tested, but would result in an η_e greater than 98%. Results from the expulsion tests in the other orientations also showed good agreement with computer predictions. The $+X$ down tests showed a differential between predicted and measured η_e of 3.5%, attributed to the difficulty in modeling the flow network for this orientation. This value was within 1.5% for the tests in the other three orientations, which was well within test uncertainties and geometric deviations of the model from the full-scale design. Comparing scaled results with full-scale predictions also showed good agreement. For $+X$ up orientations, high-mode η_e of 97.8% and 98.3% resulted for the subscale model and full-scale prediction, respectively. Comparable results for the $+Z$ up orientation were 94.6% and 96.3%, respectively. These differences were also attributed to test uncertainties and model geometric deviations.

Both pulsed flow only and pulsed and steady flow combined were used to assess the impact of start-up and shutdown transients on acquisition system operation. The nominal valve duty cycle of 40 msec open and 40 msec closed with a 20-msec opening and closing time simulated RCS valve response and maximum thruster cycling. No effect of pulsed flow was observed except for the case when liquid was outflowed at rates in excess of scaled values, against an adverse acceleration, and the volume of liquid was small.

Centrifuge testing was performed with Freon TF to evaluate high-g RTLS abort and re-entry operations. For the RTLS simulations, liquid residual ranged from 34 to 42%. At the scaled flowrate, the liquid remaining was 38%, which exceeded the original 34.5% of load requirement but was far beyond the revised 65% level. The re-entry simulations showed that 98% η_e could not be achieved due to screen dryout and subsequent gas pull-through in channels of both the pressurization and outlet compartments. This was true for all flowrates tested.

Vibration tests were conducted with Freon TF to determine the impact of the 1.93-g rms random vibration on acquisition system performance. This vibration results from OMS engine operation in either of two modes which could affect the RCS. The first is the pure hydrostatic effect during firing of both OMS engines with no RCS operation, and the second is an OMS engine-out condition requiring firing of four RCS thrusters for roll control. Tests covered a range of random vibrations. Results showed general agreement with hydrostatic theory.[3,4] Expulsion tests indicated little difference in η_e between steady one-g and random vibration tests. Outflow to the 4% level exceeded the 13% level below which OMS roll control would not be performed.

Slosh testing with IPA showed that the barrier/channel system acts as a slosh baffle providing five to seven times the

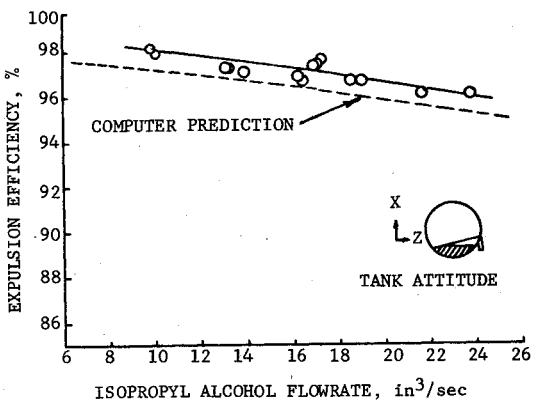

Fig. 4 Comparison of measured and predicted performance of ⅓ scale model

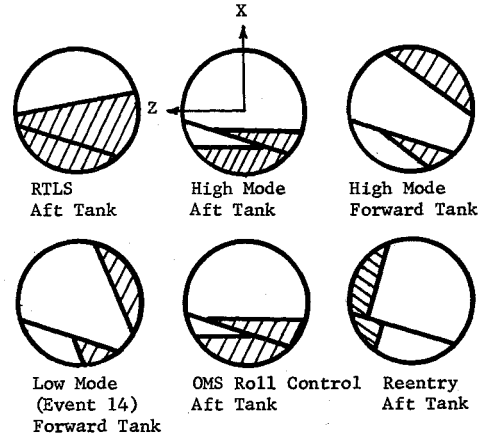

Fig. 5 Critical mission event liquid orientation.

damping of a bare sphere. The low-g tests used high density FC-43 fluorocarbon solvent as the test fluid. Results showed that the probability of liquid reorienting through the center of the tank was low and that, if it did occur, sufficient liquid would remain in contact with the screen channels to maintain continuous liquid feed during this transient condition.

Design Impact

The verification testing showed the need for design modification in two areas, tank filling and re-entry expulsion. Vent tubes were needed to minimize trapped gas during fill with wet screens and bubble filters were needed to prevent gas pull-through during re-entry. Also, screen area was increased for RTLS and re-entry operations to reduce liquid residual at breakdown.

Full-Scale Tankage Evaluation

Design and Fabrication

Detail design of the full-scale surface tension system was based on the subscale design verification results and revised criteria. The updated criteria more closely aligned the technology and flight hardware programs by requiring an expulsion efficiency of 98%, a design safety factor on bubble point of 1.15, 65% of load cutoff for RTLS, and 13% of load cutoff for all high mode operations (low mode tank depletion). Twenty-four possible RCS mission events were specified, of which six were considered as critically influencing systems design. Liquid orientation during these six events is shown in Fig. 5, assuming settled propellant, flat-interface conditions. The tank Bond Number is sufficient to produce a flat liquid/vapor interface.

The resulting acquisition system design is shown schematically in Fig. 6. The propellant tank shell is divided into a larger pressurization compartment and a smaller outlet compartment by a solid barrier. Pressurant enters the pressurization compartment and propellant feeds from this compartment through a total communication type of channel network (pressurization compartment screen channels and ring manifold), through the pressurization compartment manifold screen bubble filter, and into the bulk region of the outlet compartment. From there, the propellant flows into and through another channel network (outlet compartment screen channels and ring manifold), into and through the sump screen bubble filter, and into the screen re-entry sump to the tank outlet. If propellant in the pressurization compartment contacts the screen re-entry collector, it can also feed through this component directly into the outlet compartment bulk region. Also, if propellent is in contact with the re-entry sump, it can feed directly through this screen component to the outlet. The design accommodates two-phase flow from the pressurization compartment while assuring only single-phase liquid feed to the outlet.

Only a single-layer screen is used throughout the design. A finer mesh screen is used for all channel, manifold, collector, and sump capillary components than is used for the two bubble filters. The former is a 325×2300 mesh Dutch-twill screen. Because this fine mesh screen is made of 304L stainless steel, all capillary components, including channel sides and screen support structure, are fabricated of this material, due to joining considerations.

Under the high re-entry acceleration, the screen can dry out, allowing gas to flow into the channels. The two bubble filters were added to prevent premature gas pull-through from the pressurization compartment into the outlet compartment and from the outlet compartment into the outlet. This necessitated the addition of a separate flow path from the pressurization compartment to the outlet compartment (re-entry collector) and from the outlet compartment to the outlet (re-entry sump).

The prototype flight design includes an inclined solid barrier tilted up toward the $+Z$ axis. All barrier penetrations

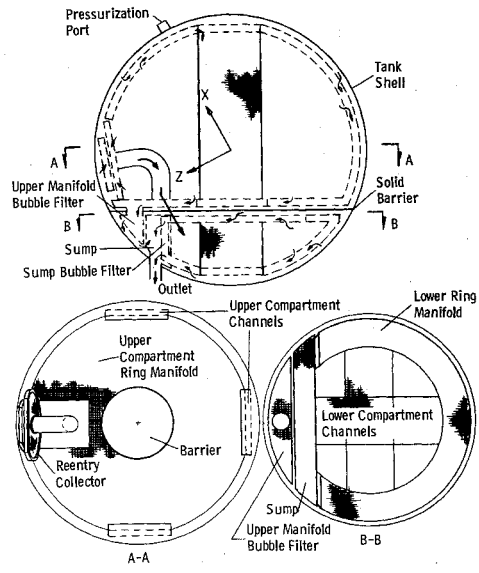

Fig. 6 Full-scale design

(two) are limited to the $+Z$ side of the barrier. This allows the tank outlet to be positioned in the outlet compartment in the re-entry puddle under the barrier. Computer optimized channels are employed, with a common design used in both compartments. Considerations included the number, cross section, aspect ratio, and screen mesh required to maximize both low-g on-orbit expulsion efficiency and high-g re-entry expulsion efficiency. The impact that the critical mission events had on system design is noted in Table 1. The pressurization compartment ring manifold has screen on both its upper and lower surfaces to decrease liquid entry pressure drop and increase the quantity of liquid that can be transferred as two-phase to the outlet compartment. This manifold stands away from and provides support for the solid barrier, which is welded to the tank shell (allowing the tank and barrier to be constructed of same material, e.g., 6A1-4V titanium). With a titanium tank and stainless steel surface tension device, the transition is made using mechanical seals where the stainless steel tubular flow paths penetrate the titanium barrier.

Bubble filters are incorporated in the liquid flow paths to prevent premature gas pull-through during re-entry, and an enlarged screen surface component is included in both compartments. These components are the re-entry collector and the re-entry sump. Both are necessitated by the bubble filters and both are located on the $+Z$ side of the tank in the re-entry puddle in each compartment. These four components are needed to meet the high-g re-entry requirements and could be eliminated from a system which did not need to outflow during re-entry (on-orbit, low-g depletion only).

The all-metal surface tension design was fabricated as an all-welded system, except for the barrier penetration mechanical seals. Resistance welding was used for screen-to-plate attachment and fusion welding was used to join plate material. Lateral support plate across the channel forms a ladder-type structure to which the screen is attached. This technique provides a strong, lightweight structure. Bleed lines were incorporated at the high point of all capillary components to vent gas trapped by wet screen during fill. The outlet compartment channel system is shown in Fig. 7, and the pressurization compartment components are shown installed in the ground test tank in Fig. 8. Bleed lines can be seen in each figure; the solid barrier is visible beneath the ring manifold in Fig. 8. The feasibility of a welded tank/barrier assembly using mechanical seals at the barrier penetrations was demonstrated. Total weight of the acquisition system, including the solid barrier, was 25 lbm. Acceptance testing of as-received screen, parts, subassemblies, and the total system prior to tank closure was accomplished by measuring bubble

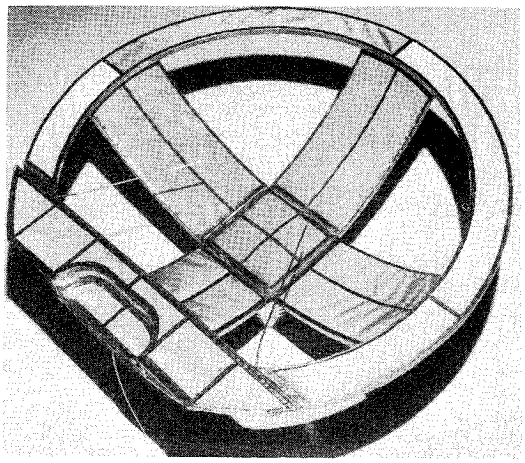

Fig. 7 Outlet compartment channel system

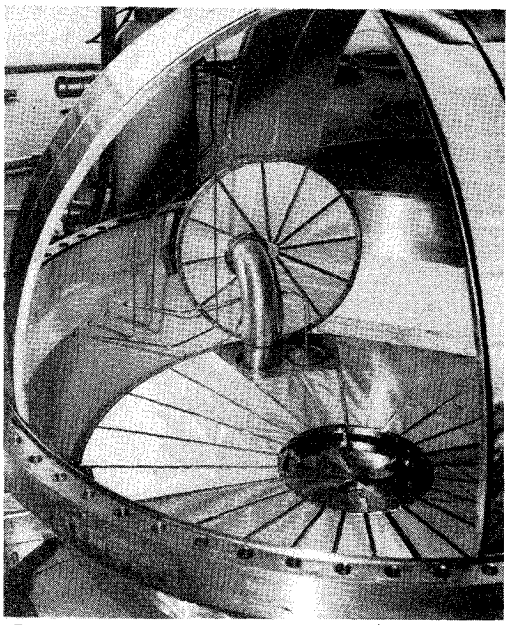

Fig. 8 Pressurization compartment channel system and re-entry collector

point. Particulate count from effluent samples taken during assembled tank flush operations showed that the necessary cleanliness level can be provided using reasonable care during fabrication.

Ground Testing

The full-scale tankage ground test program was conducted to verify cleaning, fill and drain, and inspection procedures. In addition, 1-*g* outflow tests were conducted to simulate RTLS abort and re-entry operations and an adverse 1-*g* expulsion simulated a $+Z$ orbital maneuver. The tests were conducted with IPA, MMH, and N_2O_4.

Fill and drain tests were performed with IPA to evaluate vertical fill and vertical and horizontal drain procedures and to determine the need for vent tubes during filling. The vertical attitude corresponds to tank orientation when the Orbiter is in launch position, while the horizontal attitude results after landing. Tank filling was accomplished at 10 gpm with no problems encountered with initially dry screens or with the bleed lines vented. The fill rate was limited to 5 gpm with initially wet screens and no bleed-line venting. Considerable gas was trapped during filling, particularly with wet screens. Results showed that bleed lines connected to the high points of all components are required for fill, except for the pressurization compartment channels, which trapped little

Table 1 Impact of critical mission events on full-scale design

Critical mission event	Primary impact	Secondary impact
On-orbit low-mode (event 14)	1) channel 2) screen mesh 3) Outlet compartment	1) re-entry sump and bubble filter
On-orbit high-mode and OMS roll control		1) channel 2) screen mesh 3) outlet compartment 4) pressurization compartment ring manifold
RTLS abort	1) barrier location 2) pressurization compartment ring manifold	1) re-entry collector 2) manifold filter
Re-entry	1) re-entry collector 2) manifold bubble filter 3) re-entry sump 4) sump bubble filter 5) barrier location	

Table 2 Outflow test results

Event simulated	Test liquid	Expulsion efficiency
Vertical drain	IPA	96.5% gas free 98.0% total
Horizontal drain	IPA	97.7% gas free 99.0% total
Re-entry	IPA	97.8%
	MMH	96.4%
	N_2O_4	98.4%
RTLS	MMH	65% gas free (some gas entered outlet compartment)
$+Z$ orbital maneuver	N_2O_4	(premature breakdown—see text)
Re-entry	N_2O_4	98.9%—gas free following breakdown in preceding test

gas. The bleed lines are particularly required for filling the outlet compartment. Procedures were verified for vertical and horizontal drain with 98% expulsion in vertical and 99% expulsion in the horizontal positions with an IPA drain rate of 10 gpm and using gas blow-through for the final 1% (see Table 2).

Considerable progress was made in establishing remote inspection/checkout procedures. Both tank draining and bubble point techniques with remote measurement of ΔP across the screens were employed. The bleed lines were used for pressure sensing, another benefit of their inclusion. The inspection tests were performed with IPA and with N_2O_4. Problems were encountered in getting to the proper wetted-screen starting condition for bubble point measurement without breaking the system down. This precluded measurement of the bubble point of the pressurization compartment components. The approach was successful for the outlet compartment components, however. The problem was aggravated with N_2O_4 because of its high vapor pressure. Spray bars to allow spray wetting are probably required to provide and maintain wetted screens for bubble point inspection tests.[5] More testing is required to establish the final techniques, however.

The outflow tests were conducted to verify different facets of the design. Initial tests were conducted with IPA; these were followed by tests with MMH and N_2O_4. The test results are summarized in Table 2. MMH was outflowed gas-free to the 65% of load level in the RTLS 1-*g* simulation. Some gas was ingested into the outlet compartment during this test, indicating some dryout of the re-entry collector.

Demonstration of 98% η_e during re-entry simulations was accomplished with IPA and N_2O_4. Only 96% η_e was obtained in the MMH re-entry test. This was attributed to the fact that the channel system is completely stable in a 1-g environment with MMH, holding additional liquid in the channels at depletion. This should not be encountered in the actual 2.2 g re-entry environment.

During the $+Z$ orbital maneuver simulation, premature breakdown occurred during the N_2O_4 outflow. This was attributed to some draining of liquid from the re-entry collector through the collector tube into the outlet compartment and subsequent collector screen dryout, with the draining caused by collector tube instability in the 1-g environment. The need for adding a 100×100 mesh screen across this opening is indicated. Even after breakdown of the re-entry collector and the initiation of gas flow through this path into the outlet compartment, N_2O_4 liquid continued to be transferred through the other flow path (channel/ring-manifold/bubble-filter path). In fact, over 100 lbm of N_2O_4 were transferred from the pressurization to the outflow compartment between the time the re-entry collector broke down and the time of outlet compartment depletion. This was a vivid demonstration of the capability to transfer two-phase flow across the barrier. Following this test, the tank was rotated into the re-entry orientation and a single-phase outflow was reestablished to 98.9% η_e. A high degree of certainty in accomplishing re-entry is indicated by this and the other re-entry tests.

Conclusions

Through a combination of analysis and subscale and full-scale testing, the fine-mesh screen, compartmented tank design showed considerable promise for meeting the demanding requirements of the omnidirection thrusting, pulsed-flow SS/RCS system. The acquisition system should be capable of performing both the high-g and low-g mission operations. Additional analysis and testing are required, however, to translate the results of this program into a fully developed flight system.

References

[1] Fester, D.A., Eberhardt, R.N., and Tegart, J.R., "Space Shuttle Reaction Control Subsystem Propellant Acquisition Technology, *Journal of Spacecraft and Rockets*, Vol. 12, Dec. 1975, pp. 705-711.

[2] Fester, D.A., "SS/RCS Surface Tension Propellant Acquisition/Expulsion Tankage Technology," Martin Marietta Corp., Denver, Colo., MCR-75-171, Aug. 1975.

[3] Warren, R.P., "Acquisition System Environmental Effects Study," Martin Marietta Corp., Denver, Colo., MCR-75-21, May 1975.

[4] Page, G.R., "Acquisition/Expulsion System for Earth Orbital Propulsion System Study, Volume III – Cryogenic Tests," Martin Marietta Corp., Denver, Colo, MCR-73-97, Vol. III, Oct. 1973.

[5] Fester, D.A., "Acquisition/Expulsion System for Earth Orbital Propulsion System Study, Volume V—Earth Storable Design," Martin Marietta Corp., Denver, Colo., MCR-73-97, Vol. V., Oct. 1973.